

The effect of radiation propagation time on fluorescence decays

Sandrina P. Barbosa, Alexander A. Fedorov, Mário N. Berberan-Santos *

Centro de Química-Física Molecular, Instituto Superior Técnico, 1049-001 Lisboa, Portugal

Received 16 December 2004; in final form 23 February 2005

Available online 23 March 2005

Abstract

The effect of the time-of-flight of the exciting and emitted photons on fluorescence decays is studied. Fluorescence decay laws are obtained for spherical and linear geometries. Experimental results for silica nanoparticles and for Rhodamine 101 solutions are analysed according to the developed model. It accounts well for the main features of the observations, the inclusion of photon propagation times being essential for a correct description of the fluorescence decays under the described circumstances. It is also shown that from the time dependence of fluorescence one can in principle determine the absorption or scattering coefficients of the sensed medium.

© 2005 Elsevier B.V. All rights reserved.

1. Introduction

The space and time scales involved in most laboratory fluorescence measurements are such that it is appropriate to neglect the finiteness of the speed of light, which is approximately 0.3 mm/ps in a vacuum, and a little less in common solvents, e.g., 0.23 mm/ps in water for visible radiation. The propagation time of radiation is on the other hand at the heart of both Rayleigh and fluorescence light detection and ranging (LIDAR) techniques [1] employed in environmental and atmospheric studies. In these techniques it is the fluorescence lifetime role that is negligible.

However, when dealing with very short time scales (femtoseconds) and/or extended laboratory systems (more than a few centimetres in linear dimension) in the nanosecond or picosecond range, both the fluorescence lifetimes and the propagation time of radiation are important.

We have previously considered the effect of the time-of-flight of the photons in a mainly qualitative way in

the context of atomic and molecular radiative transfer [2,3].

In this work, we address the effect of the time-of-flight of the photons on fluorescence decays. Fluorescence decay laws are obtained for two model geometries, one spherical, and another linear. Experimental results are obtained for the linear case, and analysed according to the developed model. It is shown that the model accounts well for the main features of the recorded decays, and that the inclusion of photon propagation times is essential for a correct description of fluorescence decays under the described circumstances.

2. Experimental

2.1. Systems studied

The systems studied were Rhodamine 101 dissolved in acidified ethanol and colloidal silica in water. Rhodamine 101 (Radiant Dyes), silica (Ludox TM-50, Aldrich) and ethanol (Merck, spectroscopic grade) were used as supplied. Silica and Rhodamine 101 concentrations were 3×10^{-4} g/ml and 3×10^{-8} M, respectively.

* Corresponding author. Fax: +351 21 846 44 55.

E-mail address: berberan@ist.utl.pt (M.N. Berberan-Santos).

2.2. Fluorescence measurements

A glass cylindrical tube with a quartz wall, with an inner radius of 1.8 and 120 cm length was filled with the solutions. The excitation and detection geometry is shown in Fig. 1. The excitation beam, initially at a right angle with the tube, is redirected into the tube, along its axis, by means of a small mirror, located 3 cm away from the tube wall. The fluorescence emission is collected with a large lens, placed along the cylinder axis and 10 cm away from the tube end.

Time resolved picosecond fluorescence measurements were performed using the single-photon timing method with laser excitation. The set-up consisted of a mode-locked Coherent Innova 400-10 argon-ion laser that synchronously pumped a cavity dumped Coherent 701-2 dye (Rhodamine 6G or DCM) laser, delivering fundamental or frequency-doubled 5 ps pulses at a repetition rate of 3.4 MHz, or alternatively, of a Spectra-Physics Millennia Xs Nd:YVO₄ diode pumped laser, pumping a pulse picked Spectra-Physics Tsunami titanium-sapphire laser, delivering 100 fs frequency-doubled pulses at a repetition rate of 4 MHz. Intensity decay measurements were made by alternate collection of impulse and decay, with the emission polarizer set at the magic angle position. Impulse was recorded slightly away from excitation wavelength with a scattering suspension (1 cm cell). For the decays, a cut-off filter was used, effectively removing all excitation light. Rhodamine 101 solutions were excited at either 320 or 575 nm and silica suspensions at 415 nm. The emission signal passed through a depolarizer, a Jobin-Yvon

HR320 monochromator with a grating of 100 lines/nm, and was recorded on a Hamamatsu 2809U-01 microchannel plate photomultiplier as a detector. A time scale of 16.8 ps/channel was used for the silica sample and 30.6 ps/channel for the Rhodamine 101 samples. The instrument response function had an effective FWHM of 35 ps.

3. Model geometries

3.1. Spherical medium, with isotropic excitation source and detector in the centre

Consider a sphere of radius R_s , enclosing a smaller and concentric sphere of radius r_0 , Fig. 1a. Between these spherical surfaces is contained an absorbing and fluorescent medium with refractive index n (real part of the complex refractive index), assumed to be frequency-independent in the range of interest. Excitation radiation is isotropically emitted from the walls of the smaller sphere that also acts as detector of the medium fluorescence.

For delta excitation, and assuming at first that light attenuation by absorption is negligible (dilute solution), the fluorescence emitted at a point located at a distance r from the centre is given by

$$i(r, t) = \frac{1}{4\pi r^2} \rho(t - r/v), \quad (1)$$

where v is the speed of light in the medium and

$$\rho(t) = \exp(-t/\tau) \quad (2)$$

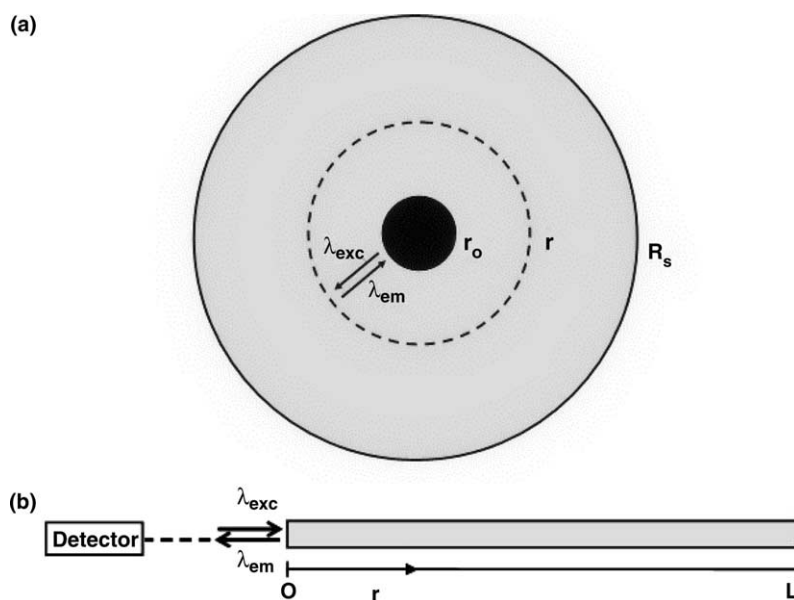


Fig. 1. (a) Spherical geometry model. Exciting radiation is emitted from the surface of the inner sphere (radius r_0) and fluorescence is detected at the same surface. (b) Linear geometry model, with excitation and detection at the same side.

and τ is the fluorescence lifetime. The fluorescence reaching the detector results from a sum of contributions from all layers. The emission from each layer that reaches the centre is $\rho(t - 2r/v)/(4\pi r^2)$, and therefore the total fluorescence reaching the detector is

$$I(t) = \int_{r_0}^{R(t)} \frac{1}{4\pi r^2} \rho\left(t - \frac{2r}{v}\right) dr, \quad (3)$$

where $R(t)$ is given by

$$R(t) = \begin{cases} r_0 + \frac{vt}{2} & \text{if } t < 2R_s/v, \\ R_s & \text{if } t \geq 2R_s/v. \end{cases} \quad (4)$$

It is assumed that $r_0 \ll R_s$. Attenuation of the excitation intensity, owing to light absorption by the fluorophore, is now accounted for by inclusion of an exponential term in Eq. (3),

$$I(t) = \int_{r_0}^{R(t)} \frac{\exp(-\beta r)}{4\pi r^2} \rho\left(t - \frac{2r}{v}\right) dr, \quad (5)$$

where β is the absorption coefficient at the excitation wavelength. Using Eq. (2), Eq. (3) can finally be rewritten as

$$I(t) = \exp(-t/\tau) \int_{r_0}^{R(t)} \frac{\exp[(2/v\tau - \beta)r]}{4\pi r^2} dr \quad (6)$$

or

$$I(t) = \exp(-t/\tau) \int_{r_0}^{R(t)} \frac{\exp(\gamma r)}{4\pi r^2} dr \quad (7)$$

with $\gamma = 2/v\tau - \beta$. It is thus seen that the decay departs from an exponential only for times shorter than $2R_s/v$, and it is for this time scale that the propagation time has an effect on the decay shape. $t_r = 2R_s/v$ is indeed a characteristic photon propagation time for the system, as it is the maximum round-trip time.

The fluorescence decay can be rewritten in terms of dimensionless parameters, and Eq. (7) becomes, apart from a multiplying factor,

$$I(t) = \exp(-t/\tau) P(t), \quad (8)$$

where the function $P(t)$ is conveniently defined as

$$P(t) = \int_0^{X(t)} \frac{\exp(\xi x)}{(x + x_0)^2} dx \quad (9)$$

and the new parameters are

$$x_0 = r_0/R_s, \quad (10)$$

$$X(t) = \begin{cases} t/t_r & \text{if } t < t_r, \\ 1 & \text{if } t \geq t_r \end{cases} \quad (11)$$

and

$$\xi = t_r/\tau - \beta R_s. \quad (12)$$

The decay is thus controlled by the dimensionless parameters x_0 and ξ .

3.2. Cylindrical medium, with linear excitation source and a point detector outside, away from the boundary

The model geometry considered in the preceding Section 3.1 is the simplest situation possible, but is not a common one. A more realistic case occurs when the detector is located outside the medium, usually at a considerable distance from the boundary. We shall now address the quasi-one-dimensional case depicted in Fig. 1b, where excitation is linear (light beam originating from the boundary) and occurs along the symmetry axis.

For delta excitation, the fluorescence emitted at a point located at a distance r from the boundary is given by

$$i(r, t) = \frac{\exp(-\beta r)}{4\pi(r+h)^2} \rho(t - r/v), \quad (13)$$

where $\rho(t)$ is given by Eq. (2) and h is the distance from the boundary to the detector. If h is very large, one can neglect the dependence on r of the denominator in Eq. (13). The total fluorescence reaching the detector is therefore

$$I(t) = \int_0^{R(t)} \exp(-\beta r) \rho\left(t - \frac{2r}{v}\right) dr \quad (14)$$

where $R(t)$ is given by

$$R(t) = \begin{cases} vt/2 & \text{if } t < 2L/v, \\ L & \text{if } t \geq 2L/v \end{cases} \quad (15)$$

and the origin of times chosen to coincide with the excitation flash. The extra delay corresponding to the transit time of the photons outside the medium is not considered, as it is a constant common to all photons. Using Eq. (2), Eq. (14) becomes, after renormalization,

$$I(t) = \begin{cases} N \left(e^{-\frac{\beta vt}{2}} - e^{-t} \right) & \text{if } t < t_r, \\ N \left[e^{\left(\frac{2}{t_r} - \beta\right)L} - 1 \right] e^{-t} & \text{if } t \geq t_r \end{cases} \quad (16)$$

with $t_r = 2L/v$, which is again the maximum round-trip time, and with a normalization coefficient

$$N = \frac{1}{\left(\frac{2}{\beta v} - \tau\right)(1 - e^{-\beta L})} \quad (17)$$

chosen so that $\int_0^\infty I(t) dt = 1$. One clearly has

$$N = \begin{cases} v/(2L) & \text{if } \beta L \ll 1, \\ -1/\tau & \text{if } \beta L \gg 1, \end{cases} \quad (18)$$

hence the rise-time component in Eq. (16) ($t < t_r$) can display either the intrinsic lifetime of the fluorophore or an effective lifetime $2/\beta v$, whichever the smaller.

The effect of the absorption coefficient β at the excitation wavelength on the fluorescence decay is shown in Fig. 2 in terms of reduced parameters. For a small absorption coefficient ($\beta v \tau \ll 1$), the initial rising phase

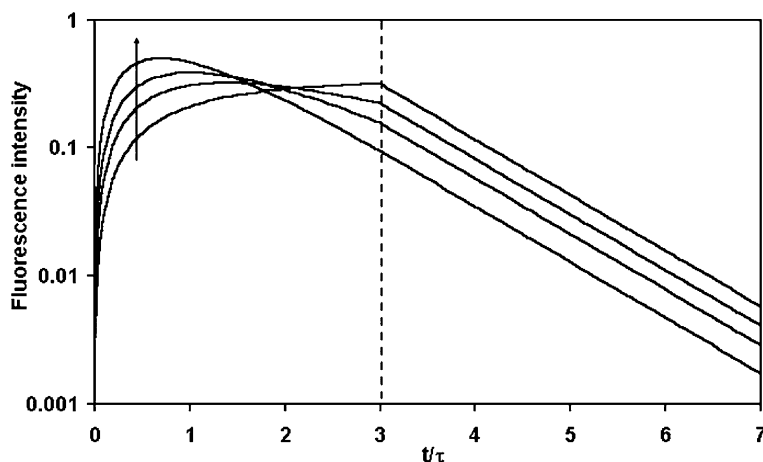


Fig. 2. Time evolution of the fluorescence intensity according to Eq. (16), with $t_r/\tau = 2L/v\tau = 3$. Curves vary with the dimensionless parameter $\beta v\tau/2$ according to the arrow. $\beta v\tau/2$ takes the values 0, 0.5, 1 and 2.

is clearly seen, with a rise-time τ . A break occurs at t_r , and from then on, the decay is single exponential, again with lifetime τ . As β increases, the break becomes less apparent, and the maximum of the decay occurs at times smaller than t_r . For a sufficiently large β , the decay is essentially single exponential from the very beginning, owing to the fact that only fluorophores located very near the boundary absorb light and can thus contribute significantly to the decay.

For short lifetimes it results from Eq. (16) that a small rise period is followed by an exponential decay with lifetime $2/\beta v$, up to t_r , after which there is a very fast decay to zero. In the extreme cases of pure Mie or Rayleigh scattering (in the single scattering regime) the rise period is essentially nonexistent, but there is also an exponential decay up to t_r , and a most abrupt drop

to zero afterwards. However, the effective lifetime is now $1/\beta v$. In fact, resonance radiation will be attenuated by scattering in both the ingoing and outgoing paths, unlike fluorescence, assumed to proceed unimpeded towards the detector.

4. Experimental decays

Experimental decays were recorded with the set-up described in Section 2, approaching the quasi-one-dimensional geometry treated in Section 3.2.

A dilute colloidal dispersion of silica nanoparticles (38 nm diameter, determined by dynamic light scattering) in water was first studied. The time dependence of the back scattered light is shown in Fig. 3. The first

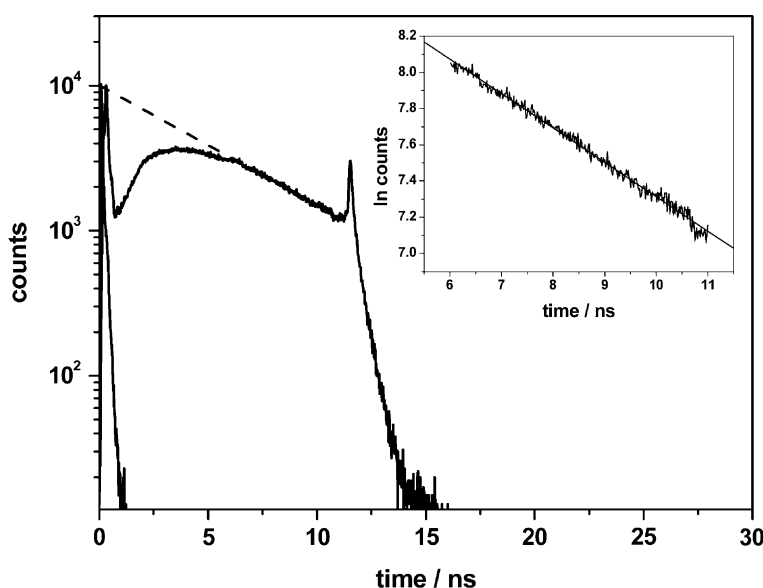


Fig. 3. Time evolution of back scattered resonant light in response to excitation at 415 nm, for a suspension of silica nanoparticles arranged according to the set-up of Fig. 1. The dashed line corresponds to the initial time behaviour predicted by the model. The inset shows the single exponential fit.

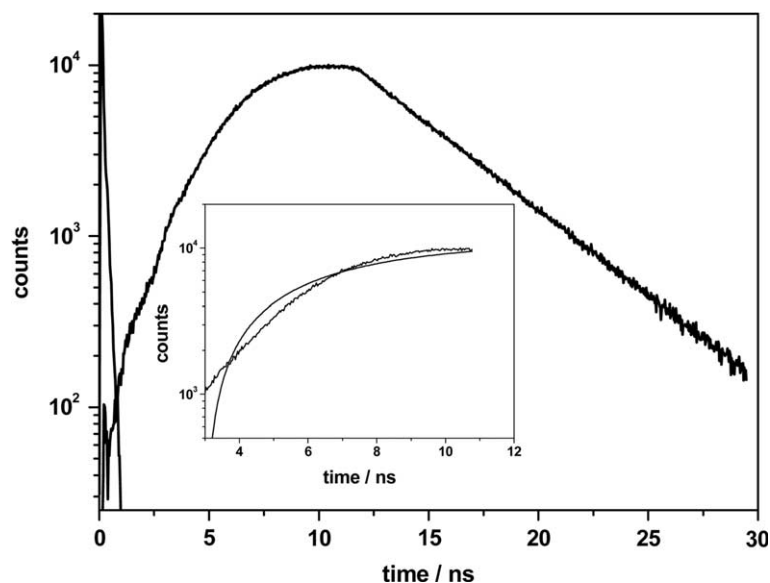


Fig. 4. Time evolution of fluorescence at 610 nm in response to excitation at 320 nm, for a Rhodamine 101 solution in the set-up shown in Fig. 1b. The inset shows the two-exponential fit.

maximum corresponds to the reflection of the laser light beam at the first wall, and the second maximum to the reflection of the laser light beam at the end wall of the tube. The second reflection occurs 11.2 ns after the first one. From this delay and a refractive index of 1.33, an effective tube length of 126 cm follows, in good agreement with the known linear dimension. The signal profile between the two reflections is clearly exponential after 6 ns. According to the model developed in 3.2, the respective time constant is $1/\beta v$. The measured value is 5.3 ns, corresponding to an extinction coefficient of $8.4 \times 10^{-3} \text{ cm}^{-1}$. This is in good agreement with the value directly measured by static light scattering

($7.3 \times 10^{-3} \text{ cm}^{-1}$) that leads to a time constant of 5.9 ns. An abrupt drop of the signal after the second reflection is also observed in Fig. 3, as predicted. The experimental curve is not single exponential for times shorter than 5 ns, as expected from the model, owing to the mask effect of the mirror placed at the entrance of the tube, that decreases the number of collected photons at short times.

The second system studied was a dilute solution of Rhodamine 101 in ethanol. The time evolution of the fluorescence in response to flash excitation (35 ps pulse width) at 320 nm is shown in Fig. 4. A first phase of rising intensity is clearly seen, up to a time of 11.9 ns,

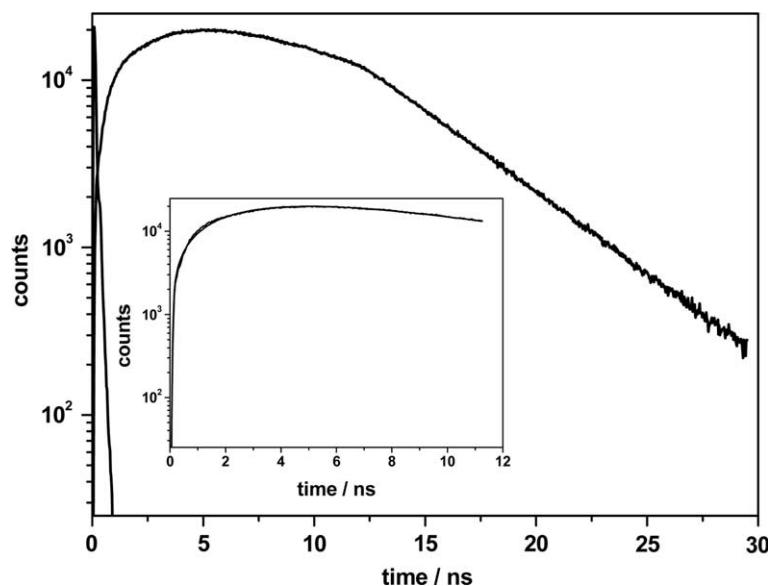


Fig. 5. Time evolution of fluorescence at 610 nm in response to excitation at 575 nm, for a Rhodamine 101 solution in the set-up shown in Fig. 1b. The inset shows the two-exponential fit.

at which the intensity starts to decay exponentially, with a lifetime of 4.3 ns, which is the known fluorescence lifetime of Rhodamine 101. The observed curve resembles the curve shown in Fig. 2 for negligible absorption ($\beta v\tau/2 = 0$). The rising portion, when fitted with a sum of two exponentials (Eq. (16)) of which one fixed at the intrinsic lifetime (4.3 ns) gives identical and symmetrical amplitudes, and a second lifetime of 457 ns, in reasonable agreement with a predicted value of 407 ns, and yielding $\beta v\tau/2 = 0.0094$. The 11.9 ns time was already encountered in the previous experiment with the silica colloidal dispersion, and is the radiation round-trip time. The fit of the model to the experimental curve is not perfect, as can be seen in Fig. 3, owing mainly to residual internal reflections that were minimized but not completely eliminated.

When selecting a second excitation wavelength, 575 nm, Fig. 5, for which the absorption coefficient is 37 times higher than at 320 nm, the first phase of the decay changes significantly, with the maximum shifted to shorter times, while the point at which the decay become single exponential (ca. 12.4 ns) remains essentially the same, as it corresponds to a common round-trip time. This is the behaviour expected and displayed in Fig. 2. The first phase of the decay, when fitted with a sum of two exponentials (Eq. (16)) of which one fixed at the intrinsic lifetime (4.3 ns) gives identical and symmetrical amplitudes, and a second lifetime of 6.2 ns (implying $\beta v\tau/2 = 0.66$), in fair agreement with the expected value of 11.0 ns.

5. Conclusions

The effect of the time-of-flight of the photons on fluorescence decays was addressed. Fluorescence decay laws

were obtained for two model geometries (spherical and linear), but the developed approach is easily extended to other geometries. Experimental results were obtained for the linear geometry, and analysed according to the developed model. It was shown that the model accounted well for the main features of the observations, the inclusion of photon propagation times being thus essential for a correct description of the fluorescence decays under the described circumstances. The measurements carried out also show that from the time dependence of fluorescence one can in principle determine the absorption or scattering coefficients of the sensed medium. While the systems studied were fairly large (in the meter range) and the time scales were in the nanosecond range, it seems clear that radiation propagation times cannot also be neglected in millimetre-sized systems when times shorter than a few picoseconds are concerned.

Acknowledgments

This work was supported by Fundação para a Ciência e a Tecnologia (FCT, Portugal) within project POC-TI/34836/FIS/2000. S.P.B. was supported by a doctoral grant from FCT.

References

- [1] R.M. Measures, *Laser Remote Sensing: Fundamentals and Applications*, Krieger, Florida, 1992.
- [2] M.N. Berberan-Santos, E.J. Nunes Pereira, J.M.G. Martinho, *J. Chem. Phys.* 103 (1995) 3022.
- [3] E.J. Nunes Pereira, J.M.G. Martinho, M.N. Berberan-Santos, *Phys. Rev. Lett.* 93 (2004) 120201.